PROCEEDINGS, 42nd Workshop on Geothermal Reservoir Engineering
Stanford University, Stanford, California, February 13-15, 2017
SGP-TR-212

Direct Downhole Temperature Measurement and Real Time Pressure-Enthalpy Model Through Photon Counting Fibre Optic Temperature Sensing

Anggoro Wisaksono[123], Andrea Pizzone[1], Nathan R. Gemmell[1], Paul L. Younger[1], Robert H. Hadfield[1]

[1]School of Engineering, James Watt South Building, University of Glasgow, Glasgow G12 8QQ

[2]Indonesia Endowment Fund for Education

[3]a.wisaksono.1@research.gla.ac.uk

Keywords: geothermal, brine, H_2O-NaCl, two-phase, fibre optics sensor, temperature sensing.

ABSTRACT

Temperature, pressure and enthalpy data is very important and valuable, both during geothermal drilling and in well operation. We research the possibility of direct downhole measurement of temperature, free calibration, which will result in a real time pressure and enthalpy reporting model. We report on the development of a downhole geothermal brine pressure and enthalpy model, applied to the state-space T-p-X delineations and density (ρ) correlations in flowing gas, liquid and two-phase systems, using the H_2O–NaCl geothermal brine thermodynamic formulation. The model was implemented in C programming, running in the NI Lab Windows/CVI user interface. The model is highly dependent on our fibre optic temperature sensor system for a direct temperature measurement. We are working to extend the range of an existing calibration-free fibre optic temperature sensing technique based on photon counting measurements by Raman backscatter (previously developed in collaboration with the US National Institute of Standards and Technology). We aim to extend the range of the system to kilometre length, by increasing the optical power per pulse and reducing the repetition rate of the excitation laser. We will employ superconducting single photon detectors with improved efficiency (5%) housed in a practical, closed-cycle cooling system.

1. INTRODUCTION

Temperature data plays an important role in many geothermal downhole procedures, including depth temperature profiles in well logging processes (PT and PTS logging) and real time thermal measurements to monitor the performance of producing wells (Brown, 2009; Blankenship & Finger, 2010). Recently, numerous studies have presented analyses of temperature measurement using fibre optics in monitoring temperatures in application to hydrogeology, oil and gas surveys and geothermal energy (Bolognin & Hartog, 2013). Temperature measurement using high-resolution, single-mode fibre optic distributed Raman sensors has been developed in previous research using meter-scales of fibre optic cables. We intends to extend the range of a calibration-free fibre optic temperature sensing technique based on photon counting measurements of Raman backscatter, developed in collaboration with the US National Institute of Standards and Technology by Tanner et al. (Tanner, et al., 2011; Dyer, et al., 2012) for geothermal applications in downhole temperature measurement.

In addition to temperature measurement, we also model the real-time known temperature pressure-enthalpy relationship based on directly measured temperature. Information on enthalpy conditions within wells and reservoir equip engineers with better insight into reservoir and well performance. The potential users typically need confidence that a certain geothermal field is capable to produce sufficient energy at affordable cost.

Our current goal is to obtain temperature data continuously along 1 km fibre optic cable with the obtained temperature readings input to the enthalpy measurement model application. Calibration-free fibre optic temperature sensing techniques based on photon counting measurements of Raman backscatter have been investigated recently (Dyer, et al., 2012). Most of the system was constructed from cheap fibre-optic components from the telecommunication industry, with a few less common components including filters and amplifiers. The output of the model comprises graph of depth-temperature, depth-enthalpy and pressure-enthalpy.

Section 2 will explain the theoretical context of the target geothermal fluids. Section 3 will explain the fibre optic distributed Raman temperature sensor and Section 4 will describe the prototype system. The experimental results and discussion will be at section 5 and followed by the conclusions in section 6.

2. HYDROTHERMAL FLUIDS

The hydrothermal reservoir is assumed to contain of H_2O, CO_2, H_2S and NaCl. The flow in the reservoir is assumed to be one or two phase flow, with fluid mixtures of brines, which might be H_2O with NaCl, KCl or $CaCl_2$ or sulphate waters (H_2O - SO_4) or bicarbonate waters (H_2O – HCO_3).

In our present phase of research we are focusing on H_2O-NaCl geothermal brine, typical of most hydrothermal brines. In the first phase of the experiment, we will measure single-phase saturated water (H_2O), then followed by H_2O-NaCl liquids.

2.1 Saturated water (H_2O)

For the purposes of the first phase of the experiment, the programming assumes saturated water and vapour according to measurements for known temperatures. The temperature accords with equation (19) (see section 3).

The basis of the enthalpy measurement programing is the formula standard of The International Association for the Properties of Water and Steam (IAPWS). The programming is valid for properties of saturated water and steam. We use the following constants; T_{crit}= 647.096 K, p_{crit}= 22064000 Pa, ρ_{crit}= 322 kg/m^3, α_0= 1000 J/kg, $\phi_0 = \alpha_0/T_{crit}$, $\theta = T/T_{crit}$ and $\tau = 1 - \theta$. We use linear interpolation of the steam thermodynamic table for our model validation.

At given temperature, pressure of saturated liquid (p_w) can be approximated using coefficient values through the following formulae:

$$p_w = p_{crit} e^{\frac{T_{crit}}{T}[a_1\tau + a_2\tau^{1.5} + a_3\tau^3 + a_4\tau^{3.5} + a_5\tau^4 + a_6\tau^{7.5}]} \quad (1)$$

$$\frac{dp_w}{dT} = \left(\frac{-p_w}{T}\right)\left[ln\left(\frac{p_w}{p_{crit}}\right) + b_1 + 1.5b_2\tau^{0.5} + 3b_3\tau^2 + 3.5b_4\tau^{2.5} + 4b_5\tau^3 + 7.5b_6\tau^{6.5}\right] \quad (2)$$

At any given temperature, the specific enthalpy of saturated liquid can be approximated through the following:

$$h_{wliquid} = \alpha + \frac{T}{\rho_{liquid}} \frac{dp}{dT} \quad (3)$$

The specific enthalpy of saturated gas can be solved using the following:

$$h_{wgas} = \alpha + \frac{T}{\rho_{gas}} \frac{dp}{dT} \quad (4)$$

Where α and the density (ρ) using the following:

$$\alpha = \alpha_0[b_0 + b_1\theta^{-19} + b_2\theta + b_3\theta^{4.5} + b_4\theta^5 + b_5\theta^{54.5}] \quad (5)$$

$$\rho_{wliquid} = \rho_{crit}\left[1 + c_1\tau^{\frac{1}{3}} + c_2\tau^{\frac{2}{3}} + c_3\tau^{\frac{5}{3}} + c_4\tau^{\frac{16}{3}} + c_5\tau^{\frac{43}{3}} + c_6\tau^{\frac{110}{3}}\right] \quad (6)$$

$$\rho_{wgas} = \rho_{crit} e^{\left[d_1\tau^{\frac{1}{3}} + d_2\tau^{\frac{2}{3}} + d_3\tau^{\frac{4}{3}} + d_4\tau^3 + d_5\tau^{\frac{37}{6}} + d_6\tau^{\frac{71}{6}}\right]} \quad (7)$$

	0	1	2	3	4	5	6
a		-7.8595178	1.8440826	-11.7866497	22.6807411	-15.9618719	1.80122502
b	-1135.9056277	-0.0000000565134998	2690.66631	127.287297	-135.003439	0.981825814	
c		1.99274064	1.09965342	-0.510839303	-1.75493479	-45.5170352	-674694.45
d		-2.03150240	-2.68302940	-5.38626492	-17.2991605	-44.7586581	-63.9201063

Table 1. Coefficient values for saturated water pressure and enthalpy

We developed computer program based on the above formulae in C language. We use the LabWindows/CVI user interface to run the program. The user interface then produced temperature-depth and enthalpy-depth graph, based on the Raman temperature sensor readings.

2.2 H_20-NaCl brine

After the preceding development for saturated water, we proceeded to further develop the model for H_20-NaCl brine. We extended the saturated model by adding formulations for state-space T-p-X delineations and density (ρ) correlations for flowing gas, liquid and two-phase systems for geothermal brine, following Palliser and McKibbin (1998). The programming formula are limited to geothermal brine in T ≤ 647.096 K.

The saturated brine pressure (p_{brine}) formula is as follow, where $t = (T/374)^2$:

$$p_{brine} = e_1 t + e_2 t^2 + e_3 t^3 + e_4 t^4 + e_5 t^5$$

The saturated static enthalpies for saturated liquid ($h_{liquid\,SAT}$) and gas ($h_{gas\,SAT}$) geothermal brine are:

$$h_{liquid\,SAT}(T) = f_0 + f_1 T + f_2 T^2 + f_3 T^3 \quad (8)$$

$$h_{gas\,SAT}(T) = g_0 + g_1 T + g_2 T^2 + g_3 T^3 \quad (9)$$

Meanwhile for two phase flow brine liquid enthalpy (h_{l2p}), for T ≤ 647.096 K

$$h_{l2p} = h_{wliquid} + \left[h_{liquid} - h_{wliquid}\right]\left[\frac{p_w - p_{2p}}{p_w - p_{brine}}\right]^{\frac{1}{1.4}} \quad (13)$$

Two phase flow brine vapour enthalpy (h_{gs}), for T ≤ 647.096 K

$$h_{g2p} = h_{wgas} + \left[h_{gas} - h_{wgas}\right]\left[\frac{p_w - p_{2p}}{p_w - p_{brine}}\right]^{\frac{1}{1.7}} \quad (14)$$

However, in two phase systems in order to get the value of enthalpy, we need to determine the downhole two-phase pressure (p_{2p}). Therefore in this model, we took the pressure value samples from the existing two phase systems.

	0	1	2	3
m	0	3.57384	-0.00379475	0.00159816
n	2500	2.85416	-0.00799981	0.00000889497

Table 2. Coefficient values for saturated geothermal brine pressure and enthalpy

3. FIBER OPTIC RAMAN DISTRIBUTED SENSOR

The sensors make use of optical time-domain reflectometry, in which measurements typically employ a pulsed source and determine position information from backscattered photons from the tested fibre. The experiment is well justified by the link between Raman backscattering and temperature that has been already demonstrated. The Stokes and anti-Stokes contribution to the total backscattering can be approximated as follows (Dyer, et al., 2012):

$$I_u = \eta_u \Delta v_u P_0 L |g_R| N(\Omega_{up}) D_c \quad (15)$$

where I_u is the backscattered photons per second, the subscript u is either S or a for Stokes or anti-Stokes, η_u is the detection efficiency (DE) of the sensors, Δv_u is the bandwidth of the Stokes or anti-Stokes filters, P_0 is the peak pump power (Tanner, et al., 2011; Dyer, et al., 2012), L is fibre length, g_R is the Raman gain factor, D_c is the duty cycle of the pump signal, Ω_{up} is the radial frequency detuning between the pump and the mean Stokes or anti-Stokes wavelengths, and N is the phonon population as follows:

$$N = \begin{cases} \frac{1}{\exp\left(\frac{\hbar|\Omega_{up}|}{k_B T}\right)-1}, & \Omega_{up} < 0 \\ \frac{1}{\exp\left(\frac{\hbar|\Omega_{up}|}{k_B T}\right)-1} + 1, & \Omega_{up} \geq 0 \end{cases} \tag{16}$$

Detuning Ω_{up} as constant over the filter bandwidths and assuming an equal value in the Stoke and anti-Stokes case, the ratio of Stokes to anti-Stokes is given by:

$$\frac{I_S(x)-B_S}{I_{as}(x)-B_{as}} = \frac{\eta_s \Delta v_s |g_R|}{\eta_{as} \Delta v_{as} |g_R|} e^{\frac{\hbar|\Omega_{sp}|}{k_B T(x)}} \tag{17}$$

Based on equation no. 17, the temperature model developed in this technique is:

$$k_B T(x) = \frac{\hbar|\Omega_{sp}|}{ln\left(\frac{I_S(x)}{C[I_{as}(x)]}\right)} \tag{18}$$

Where $T[m]$ is the measured temperature, $\hbar$ is the reduced Planck constant, Ω_{sp} is the radial frequency, k_B is the Boltzmann constant. C is the reference temperature. Should the fibre optic temperature sensor is the initial measurement, then C will be neglected.

4. SYSTEM DESCRIPTION

We will demonstrate a high resolution single mode fibre optic distributed Raman sensor, was originally developed in 2011 (Tanner, et al., 2011; Dyer, et al., 2012). The distributed sensor for temperature, followed by geothermal brine T-p-x model, used for the experiment are OTDR. According to Tanner, et al. (2011), Raman-based OTDR sensors are already sufficient for some commercial applications, such as monitoring of oil and gas wells, and also the detection of hot spots along the steam pipes of power plants, where spatial resolution much better than 1m is required. The diagram of the assembled detectors are shown in Figure 1.

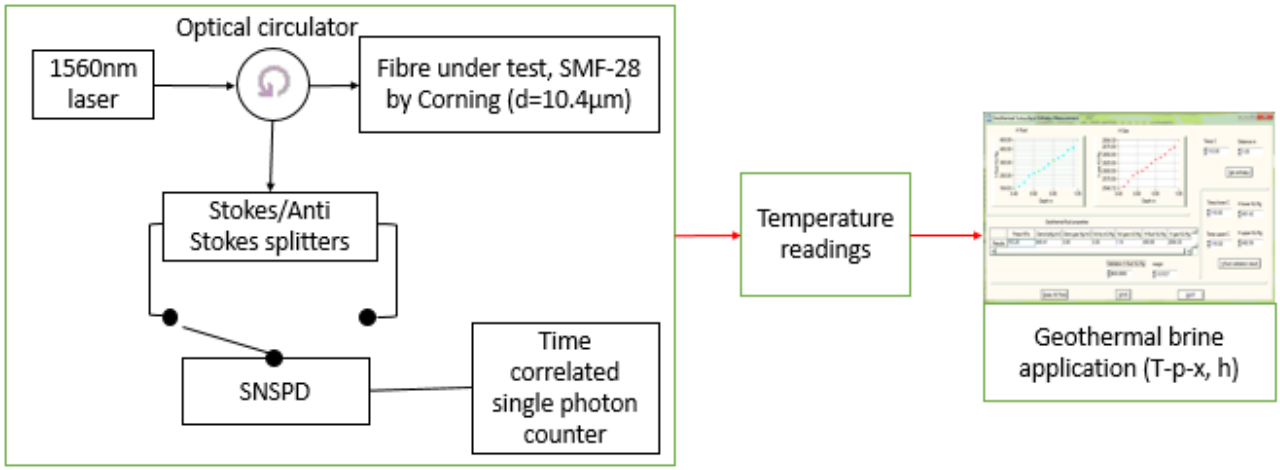

Figure 1. Simplified diagram of free calibration temperature measurement and real time pressure-enthalpy estimation.

We use femtosecond fibre laser with a spectrum near 1560 nm as source of light. The fibre under test (FUT) is standard low-loss single-mode commercial telecommunications fibre SMF28 by Corning (η = 1.452) with a mode field diameter of 10.4µm and attenuation less than 0.2 dB/km at a wavelength of 1550 nm.

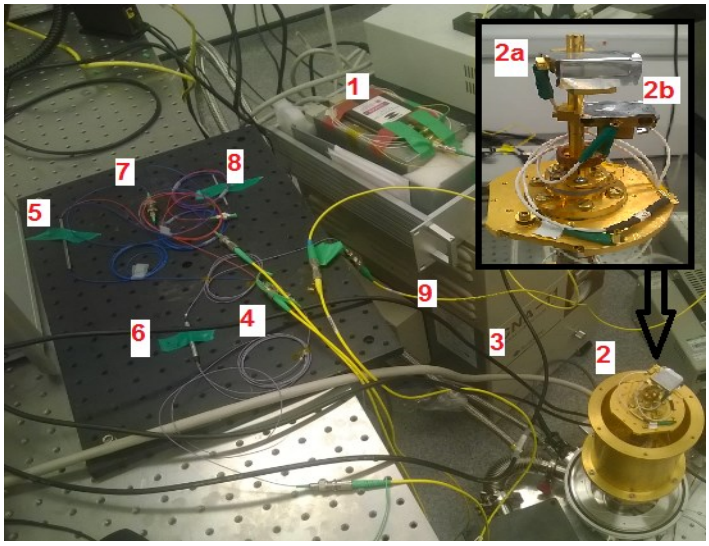

Figure 2. High resolution single mode fibre optic distributed Raman sensor experiment set up. (1) Laser, (2a and b) SNSPDs, placed inside (2) cryogenic refrigerator, (3) helium cryogenic cooler, (4) circulator, (5 and 6) splitters, (7 and 8) filters, (9) Fibre under test/FUT.

The length of the fibre is affected by the repetition rate (RR) of the pump laser that determines the period of time between each pulse. In order to get position information on the photon detected, it is required a single laser pulse. The time measured between a pulse sent into the fibre, and the scattered photon returning back down the fibre and being detected, gives the position in the fibre that the scattering happened. The more time interval there is between pulses, the more time the pulse can stay in the fibre, the longer the fibre can be. Basically, the repetition rate shall be less than 1 MHz to achieve results yet not seen in literature (Figure 2). Be l the length of the FUT and η its refractive index of the core, be c the speed of the light, the relationship is thus the following (Gold, 1985):

$$l = \frac{c}{RR*2\eta} \tag{20}$$

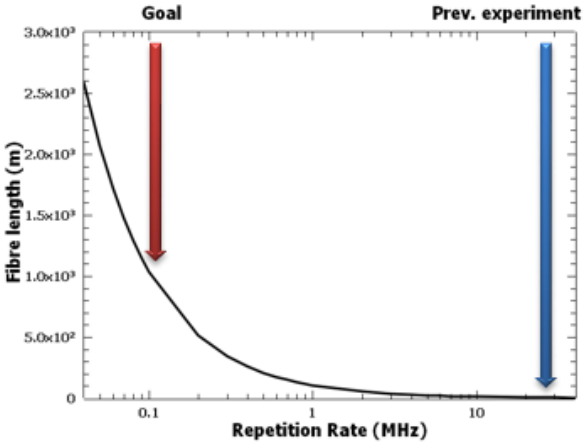

Figure 3. Extension of the fibre as a function of the RR of the pulsed laser source.

Pump filters installed before and after the fibre amplifier and attenuator. Each filter provides 25 dBm rejection of unexpected wavelengths and remove the broadband amplified spontaneous emission from the pump. The light that is backscattered from the FUT is directed by the circulator to a series of filters that have been chosen to reject the pump wavelength. Then we use S-band and L-band splitters, which are 1470 nm and 1666 nm at peak and the maximum shift is at 440 cm^{-1}. Band splitters are to separate and filter the Raman backscattered photons. The pump wavelength reject filters chosen to be approximately equally spaced between the S- and L-bands. Without these filters, we would have unwanted photons at the pump wavelength reaching our detector. The two Superconducting nanowire single-photon detectors (SNSPDs) are our photon detector. They are single-pixel meander with an active area of 15x15 μm^2. SNSPDs work properly below at extra low temperature, therefore the first operation to do is the installation of the mounted chip inside a cryostat refrigerator. The one used for the following measurements is a Gifford-McMahon cryostat, assembled by the photonic research group at the University of Glasgow, on a Sumitomo SRDK-101D-A11C helium cryogenic cooler. The lowest temperature the cryostat can reach is ~2.4 K. Then, we use time-interval analyser to create histograms of the time delays between a laser clock electrical pulse and the electrical pulses created by the detection of photons at the SNSPDs. The temperature readings then inputted to the geothermal brine model application to get the thermodynamic data for the water and then for the range of geothermal brine mixtures.

The initial experiment used water only to check the reliability of the measurement and also the model program.

5. EXPERIMENTAL RESULT

5.1 Geothermal brine application test

The coding for the saturated water model and the geothermal brine T-p-x correlation application was successfully completed, demonstrating the pressure and enthalpy in real-time when we get the temperature readings from our SPNSD sensors. Since the first test in the experiment was to measure water temperature, we had to check whether the approach is accurate.

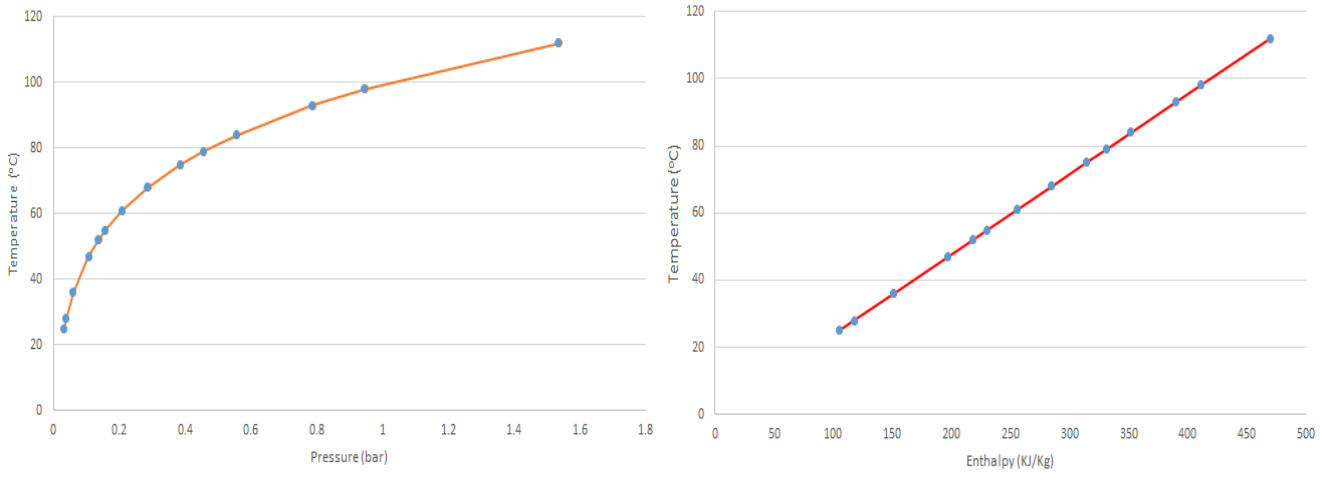

Figure 4. Application test result 1, blue dots were the readings from the application, which are align with the orange and red lines from thermodynamic steam tables.

The first test that was to ensure that the model is valid, so we compared the data output from the application with the thermodynamic saturated water tables that are commonly used. Although we obtain effectively continuous output, we approximate the temperature increase over certain spatial steps along the length of the fibre optic cable. The result are shown in figure 3, which align closely with tabulated values for saturated water.

We also simulate the application using approximate increasing distance and temperature, should it be connected with fibre optic temperature sensor and measure the water in saturated condition. We get both pressure and enthalpy as shown in figure 4. Then, we do another test in our T-p-x brine application model. The

test result is represent by figure 4. We do the similar approach by approximate the increasing temperature from 50°C up to critical point of 375°C.

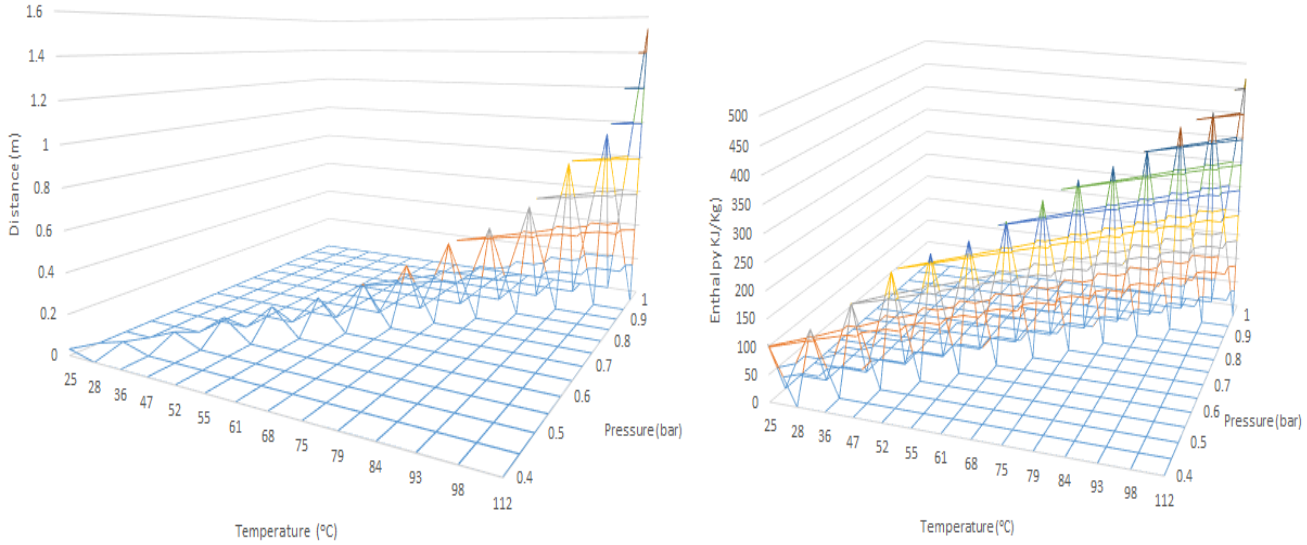

Figure 5. Application test result 2, T-p-distance and T-p-h diagram on saturated water only.

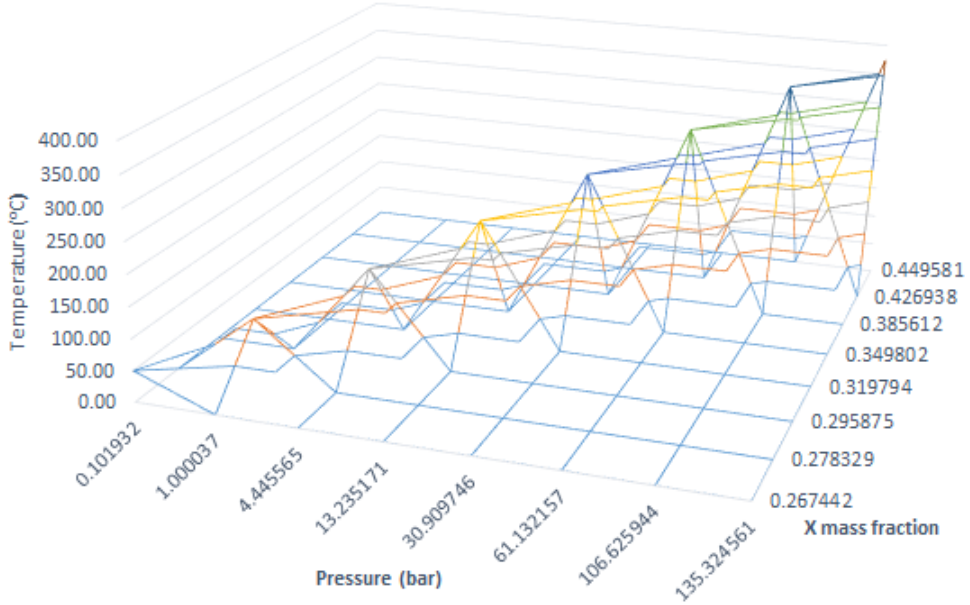

Figure 6. Application test result 3, T-p-x diagram for geothermal brine.

5.2 Temperature measurement test

The fibre under test is only 1 m long. We managed to capture the peak of temperature when put a hot water kettle in between 65-78 cm above fibre under test. It was measured approximately 65°C. The spatial resolution of 1.35 cm has been recorded. The speed of the measurement in this test recorded at 3-4 minutes. We assume, if add the geothermal brine application at the system, the overall process would no longer than 5 minutes.

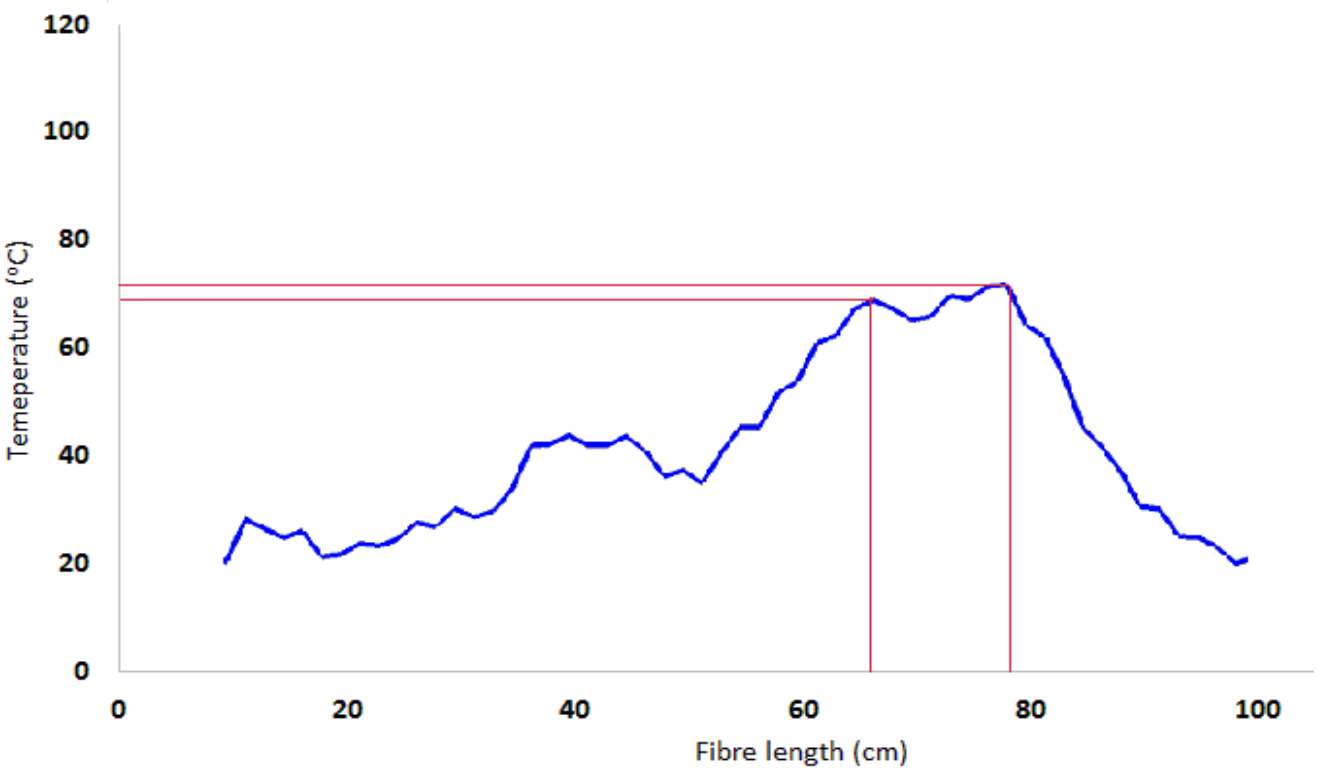

Figure 7. Temperature measurement test using 1 m fibre optic cable

Following the result of this 1 meter cable of fibre under test, we will continue with 100 m of fibre optic cable to be tested. The last experiment will be using 1 km fibre under test, before initiate the field test.

6. CONCLUSION

The initial enthalpy model result, leading up to use in conjunction with a fibre temperature set up utilising Superconductor nanowire single-photon technology currently under construction at the University of Glasgow. This will allow temperature to be measured over a kilometre of fibre, using the Raman backscattered photons.

Although laboratory testing is still ongoing at the time of writing, initial findings are vindicating the hypothesis of the real time pressure and enthalpy reporting model, from direct and free calibration downhole measurement of temperature.

Following laboratory tests using water in saturated conditions and real geothermal brine, we aim to test the tool in one of the geothermal boreholes in the north of England, to test the efficacy of our real-time pressure and enthalpy model, based on temperature sensing results, down to 1 kilometre depth and initially over the temperature interval 270 – 647K.

REFERENCES

Blankenship, D. & Finger, J., 2010. *Handbook of Best Practices for Geothermal Drilling,* Albuquerque: Sandia National Laboratories.

Bolognin, G. & Hartog, A., 2013. Raman-based fibre sensors: Trends and applications. *Optical Fiber Technology,* Volume 19, pp. 678-688.

Brown, G., 2009. Downhole temperatures from optical fibre. *Oilfield Review,* Volume 4, pp. 34-39.

Dyer, S. D. et al., 2012. Analysis of a distributed fiber-optic temperature sensor using single-photon detectors. *Optics Express,* 20(4), pp. 3456-3466.

Gold, M. P., 1985. Design of a long-range single-mode OTDR. *Journal of lightwave technology 3.1,* pp. 39-46.

Palliser, C. & McKibbin, R., 1998. A Model for Deep Geothermal Brines, I: T-p-X State-Space Description. *Transport in Porous Media,* Volume 33, p. 65–80.

Palliser, C. & McKibbin, R., 1998. A Model for Deep Geothermal Brines, II: Thermodynamic Properties – Density. *Transport in Porous Media,* Volume 33, p. 129–154.

Palliser, C. & McKibbin, R., 1998. A Model for Deep Geothermal Brines, III: Thermodynamic Properties - Enthalpy and Viscosity. *Transport in Porous Media,* Volume 33, pp. 155-171.

Pitzer, K. S., Peiper, J. C. & Busey, R. H., 1984. Thermodynamic Properties of Aqueous Sodium Chloride Solutions. *Journal of Physics and Chemistry,* pp. 1-101.

Tanner, M. G. et al., 2011. High-resolution single-mode fiber-optic distributed Raman sensor for absolute temperature measurement using superconducting nanowire single-photon detectors. *Applied Physics Letters,* Volume 99, pp. 201110-1-201110-4.